Bending Induced Rippling and Twisting of Multiwalled Carbon Nanotubes

Xiaoyan Li,[1] Wei Yang,[1,2,*] and Bin Liu[1]

[1]*Department of Engineering Mechanics, Tsinghua University, Beijing 100084, People's Republic of China*
[2]*Zhejiang University, Hangzhou 310058, People's Republic of China*

(Received 11 November 2006; published 17 May 2007)

We report that a twisting deformation mode emerges with the rippling in bent multiwalled carbon nanotubes via atomistic simulations. This mode arises from the curvature-induced lattice mismatch, and is energetically favorable. For the nanotubes with larger radii, twisting may enhance the local strain relaxation. Under the thermal fluctuation, the nucleation of defects involves bond breaking and reconstruction due to strain localization. The defective inner tubes undergo the cyclic torsion, resulting in unstable necking and even failure. Prior to fracture, a monatomic chain is formed under the combination of bending and twisting.

DOI: 10.1103/PhysRevLett.98.205502 PACS numbers: 62.25.+g, 02.70.Ns, 46.32.+x

Carbon nanotubes (CNTs) show increasing promise as components of nanoelectromechanical system (NEMS) due to their unique mechanical and electrical properties [1–7]. An in-depth investigation of the mechanical behavior of CNTs is of fundamental importance for realizing applications in NEMS devices. When multiwalled carbon nanotubes (MWCNTs) are bent [8] or twisted [6,7] repeatedly under manipulation by atomic force microscopy, their responses to large deformations suggest that nanotubes have remarkable flexibility and resistance to fracture. Recently, *in situ* observations via transmission electron microscopy [4,9,10] indicated that the ripple structures developed within bent thick MWCNTs dramatically reduced their stiffness. Such rippling mode of deformation was analyzed qualitatively by 2D finite element models with highly anisotropic elasticity [11]. The generalized local quasicontinuum simulation (QCS) revealed that the rippling of MWCNTs arose from the nonlinear effects due to the interplay of strain energy relaxation and interlayer interaction [12]. However, understanding the physical nature of nanoscale deformations and identifying the dynamics of atomic-scale activities turn out to be impossible through continuum and quasicontinuum methods. In this Letter, we provide a fully atomistic description for bending of MWCNTs via molecular dynamics (MD) at the finite temperature. The striking phenomenon observed in MD simulations is that a twisting mode occurs with corrugations because of the curvature-induced lattice mismatch [13]. Owing to the nucleation and the movement of defects under thermal fluctuations, the further development of twisting causes necking and even fracture of inner tubes prior to the failure of outer tubes.

To improve the efficiency and accuracy of calculations, we have performed MD simulations using the multiple time step algorithm [14]. During all simulations, the short time step is set as 0.5 fs and the long time step as 1.5 fs. The bonded interatomic interactions are described by a many-body Tersoff-Brenner potential [15] that allows for covalent bond breaking and forming, while the van der Waals (vdW) interactions are modeled with a Lennard-Jones potential [16] with the cutoff distance of 1.2 nm. To maintain a canonical ensemble, we adopt a Nose-Hoover thermostat [17] at room temperature (300 K). Initial equilibrium configurations are determined by the conjugate gradient method. The loading is attained by increasing the pure bending angle at both ends of the MWCNTs. In each loading step, the constrained atoms at the ends are displaced according to a bending angle increment of 0.25°, and then the system is relaxed with fixed ends for 5 ps. All simulations last 3 ns so that the bending angle is ultimately up to 150°. The considered systems are composed of single-walled to 10-walled (n, n) armchair tubes with the minimum value of $n = 5$. In all simulations for MWCNTs, the length-to-diameter ratio is maintained at 10. Accordingly, the system of single-walled CNT contains 560 carbon atoms, while the 10-walled CNTs contain 303 690 atoms.

During the bending process of MWCNTs, the geometrical transformations include the increase of curvature, the switch of cross-section shape and the occurrence of ripples. Figure 1(a) shows a longitudinal section of 10-walled CNTs with wavelike or ripple structures, which is a manifestation of geometry instability [4,9,10,12]. From the continuum mechanics perspective, bifurcations lead to nearly periodic wavelike distortions of nanotube walls [8]. The hybridization effect in the electronic structure [9,18] plays a significant role in the rippling mode. Three transversal sections shown in Fig. 1(b) describe shape switches from nearly circular section to flat-top section again to wedgelike section. These characteristic cross sections seem to imply the Brazier effect which causes the circular section to become more polygonized [8]. At the atomistic level, these transitions can be explained in terms of a model based on curvature-induced lattice mismatch

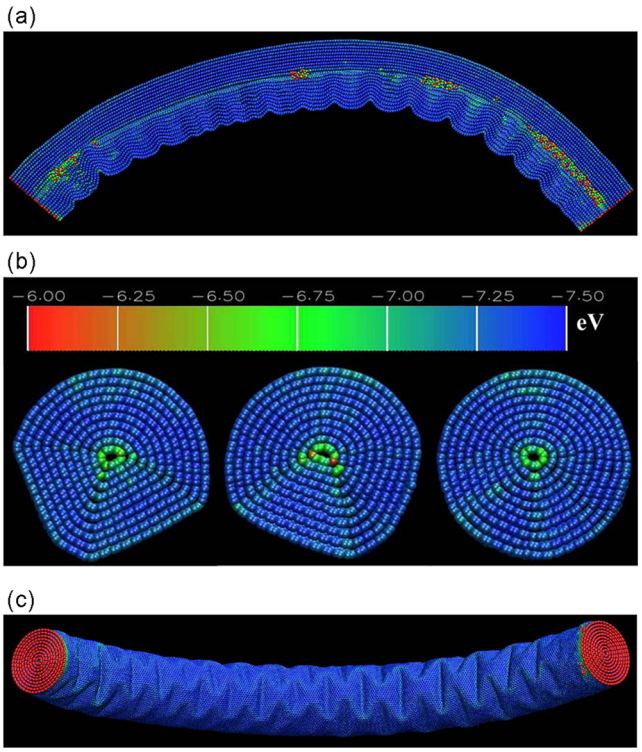

FIG. 1 (color online). Geometrical morphologies of bent 10-walled CNTs: (a) longitudinal section; (b) three characteristic transversal sections; (c) 3D configuration of deformed MWCNT. Atoms are colored according to potential energy [see color bar in (b)].

[13]. The topological morphologies depicted in Fig. 1 closely resemble the computational results obtained by QCS [12].

Fully atomistic simulations provide details in energetic dynamics unavailable from experiments and QCS. Figure 2 shows a series of images which illustrate the deformation processes of different shells. Here the shells are labeled sequentially from the innermost to the outmost shells as 0 to 9. At the beginning, MWCNTs are in an elastic regime where every shell undergoes a compression on the inner side but a stretching on the outer side. When the curvature reaches a critical value, the first wrinkle is formed in the middle of tubes due to strain buildup. Simultaneously, the bending moment drops abruptly, as shown in Fig. 3. This singularity characterizes the change of structural stability. After this initial buckling, there are obvious plastic deformations, as demonstrated by strengthening and yielding stages in the curve of bending moment versus curvature in Fig. 3. During these irreversible processes, wrinkles are progressively formed and symmetrically distributed along the nanotube walls, as a result of complicated arrangement of corrugations in Fig. 1(c). The evolution process of ripple structures is elucidated in Fig. 2(d).

Interestingly, the local portion of 0-labeled nanotube is flattened into deflated ribbons after the formation of initial wrinkles. It is attributed to interlayer torsion which stems from the lattice registry. During the bending process of MWCNTs, the successive rippling leads to the increases of surface area on bent sides and the inflection of intralayer covalent bond in local strained region. These changes introduce an effective lattice mismatch of the neighboring shells. Thus an interlayer stress is produced to recover out-of-registry atoms to in-registry positions, and that further contributes to the deformation of the tubules, e.g., generating and maintaining a twist. The 0-labeled CNT exhibits a twisted ribbonlike shape under this torsion. Additionally, vacancies and interstitials are thermodynamically nucleated near the ends where the strain localizes. Such nucleation process of defects must involve bond breaking and reconstruction. The defects seem to be pinned and cannot propagate due to small radial dimension. Under the combination of bending and twisting, the presence of defects weakens the structures and leads to early necking failure. Figure 2(a) shows two states of the innermost tube after local failure. Particularly, the innermost tube with the fixed and free ends has a twist present in the middle of tube, which is analogous to the experimental and computational observations [19]. The local segment of the fully free tube also exhibits a ribbonlike spiral, which is an apparent evidence of the twisting mode.

The central section of 1-labeled CNT undergoes slight twisting in the region which shows higher potential energy than the surrounding, as illustrated in Fig. 2(b). Concurrently, defects are formed near the ends, resulting in the local necking under the combination of bending and twisting. During the thinning process, a monatomic chain emerges by virtue of bond switching, spanning the two tube fragments. This peculiar morphological feature appears under the coupled bending-twisting mode, and is similar to a plastic behavior involving the evolution of unraveling monatomic chain when the single-walled CNT is axially stretched in several experiments and simulations [20]. For 2-labeled CNT, the localization of strain near the end of tube leads to bond rupture after the early rippling. The switching of the covalent bond promotes formation of defects under thermal fluctuations. However, the local collapse is not caused by the nucleation and development of defects. Actually, local strain is gradually released via twisting mode along nanotube wall, as demonstrated in Fig. 2(c). The corresponding interpretation is that 2-labeled CNT has a larger radius than 0-labeled and 1-labeled CNTs and provides a spiral pathway to release the local strain. At the position of defects, new networks containing five-atom, seven-atom, and eight-atom rings substitute the original hexagons, which is ascribed to bond reconstruction. Moreover, the amplitude of ripples on MWCNTs increases from the innermost tube to the outmost tube. For all of 3-labeled to 9-labeled CNTs, the sharp wavelike structures resist the twisting mode. Hence the outer tubes do not exhibit apparent twists, as shown in Fig. 2(d).

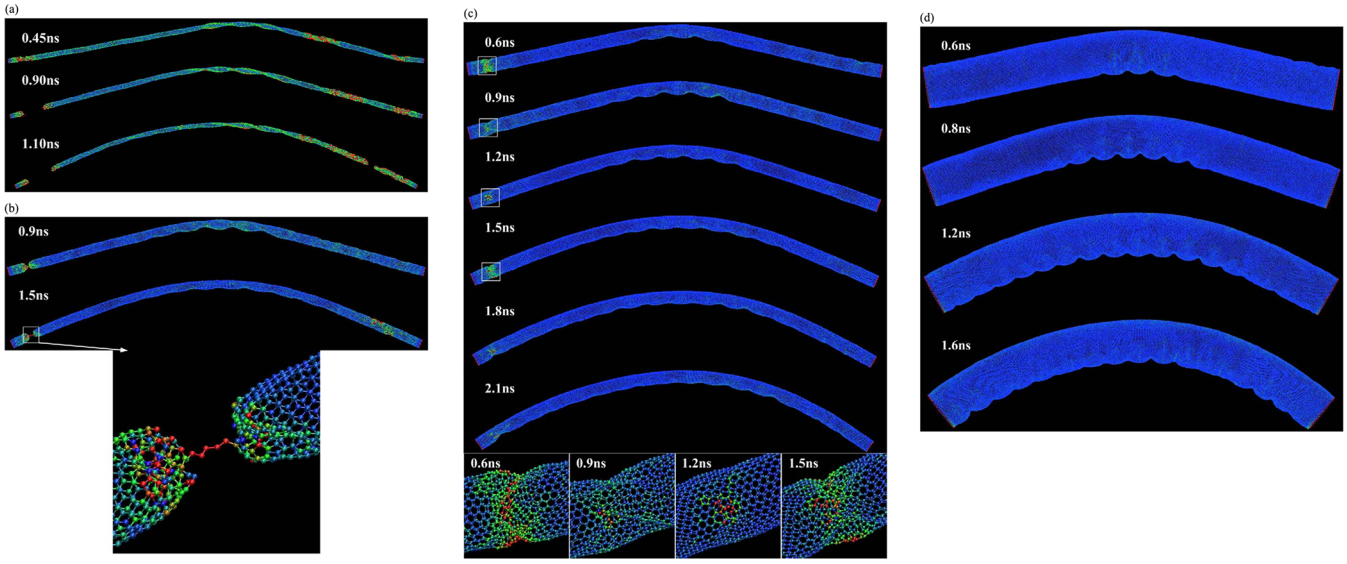

FIG. 2 (color online). Time-sequential series of snapshots for bent carbon nanotube with different shell labels: (a) thermal-activated defects are highlighted by high potential energies, and torsion causes 0-CNT to a ribbonlike flattened shape; (b) twisting mode results in necking effect and formation of monatomic chain in 1-CNT; (c) locally stored strain is released through the twisting mode, with bond breaking and reconstruction in 2-CNT; (d) rippling process of 9-CNT. Atoms are colored according to potential energy [see color bar in Fig. 1(b)].

Figure 3 depicts the bending and twisting moments as the functions of bending curvature. Here the average twisting moment is obtained by averaging torques of total atoms, and the maximal moment is recorded from torques of atoms on the cross-section with the maximum twist. When the corrugations do not appear, the average and maximal twisting moments keep almost null values. Once the rippling mode occurs, the bending moment abruptly declines due to buckling destabilization. The geometrical transformations of MWCNTs further cause the curvature-induced lattice mismatch. Here the curvature contains two aspects: one is the radial self curvature, and the other is the axial bent curvature. To minimize the potential energy and attain high commensurance, the lattice registry dependent interlayer vdW interaction arouses the twisting. During the postbuckling stage of MWCNTs, the twisting moments fluctuate due to the transient changes of chiral commensurance at the time scale of picoseconds. Under the combination of bending and twisting, the formation and development of defects lead to necking and failure of tenuous inner tubes. Notably, these phenomena are significant for applications of MWCNTs in NEMS devices. When MWCNTs are subjected to large bending deformations, the outmost tube appears to be the most critical place because it undergoes the largest duress and appears the sharpest distortion. Nevertheless, MD simulations suggest that the tenuous inner tubes locally collapse prior to the failure of the outmost tube. Furthermore, the survival of one monatomic chain before breakage morphologically resembles observations in the literature [20]. However, the present monatomic chain is formed under a coupled mode of bending and twisting that differs from the axial tensile reported in the literature [20]. This distinct plastic relaxation seems to emerge as an important topic for further studies and applications to monatomic wires as probes, emitters and connectors at the nanoscale [21].

For the present atomistic simulations, the twisting mode is related to the loading rate. However, an artificially high loading rate cannot change the underlying deformation physics in MWCNTs. The intrinsic nature of twisting is the lattice registry dependent interlayer vdW interactions. Indubitably, the chirality of MWCNTs is responsible for

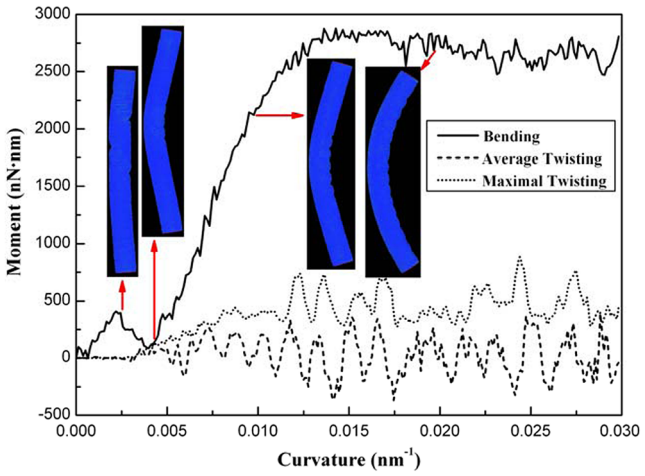

FIG. 3 (color online). Variations of the bending and twisting moments with deformation curvature for 10-walled CNTs. Four snapshots correspond to four typical points, respectively.

the occurrence of the twisting mode. The armchair tubes have so high a commensurance and ideal symmetry that the internal torsion is sufficiently activated when they confront the lattice mismatch caused by external bending load. The twisting mode is not elucidated in the investigation for bent thick MWCNTs by using QCS. The reason is that the QCS handles interatomic interactions in terms of a continuum approach (based on finite element framework) so as to ignore the lattice registry. The absence of the lattice effect further makes QCS ineffective for the defective system involving the lattice mismatch.

In summary, direct MD simulations reveal a twisting mode coupled with the rippling mode while MWCNTs undergo the bending load. The geometrical characteristics originating from large bending deformations agree well with those from experiments and QCS. The curvature-induced lattice mismatch is confirmed as a vital origin of the twisting. Under the combination of bending and twisting, the evolution of defects results in necking and failure of tenuous inner tubes. Occasionally, an unraveling monatomic chain comes into being at the later stages of failure.

This work is supported through grants by the National Natural Science Foundation of China (No. 10332020 and No. 10121202) and from the 973 Projects of China (No. 2004CB619304). The authors thank Professor Q. S. Zheng of Tsinghua University for helpful discussions, and are grateful for the supports of parallel computation on the HPCS supercomputer at the Chinese Academy of Meteorological Science.

*Electronic address: yw-dem@tsinghua.edu.cn
Email address: yangw@zju.edu.cn

[1] M. S. Dresselhaus, G. Dresselhaus, and Ph. Avouris, *Carbon Nanotubes: Synthesis, Structure, Properties, and Applications* (Springer-Verlag, Heidelberg, 2001).
[2] H. G. Craighead, Science **290**, 1532 (2000).
[3] A. N. Cleland and M. L. Roukes, Nature (London) **392**, 160 (1998).
[4] P. Poncharal, Z. L. Wang, D. Ugarte, and W. A. de Heer, Science **283**, 1513 (1999).
[5] A. Erbe, C. Weiss, W. Zwerger, and R. H. Blick, Phys. Rev. Lett. **87**, 096106 (2001).
[6] P. A. Williams, S. J. Papadakis, A. M. Patel, M. R. Falvo, S. Washburn, and R. Superfine, Phys. Rev. Lett. **89**, 255502 (2002).
[7] A. M. Fennimore, T. D. Yuzvinsky, W. Q. Han, M. S. Fuhrer, J. Cumings, and A. Zettl, Nature (London) **424**, 408 (2003).
[8] M. R. Falvo, G. J. Clary, R. M. Taylor, V. Chi, F. P. Brooks, S. Washburn, and R. Superfine, Nature (London) **389**, 582 (1997).
[9] T. Kuzumaki, T. Hayashi, H. Ichinose, K. Miyazawa, K. Ito, and Y. Ishida, Philos. Mag. A **77**, 1461 (1998).
[10] O. Lourie, D. M. Cox, and H. D. Wagner, Phys. Rev. Lett. **81**, 1638 (1998).
[11] J. Z. Liu, Q. Zheng, and Q. Jiang, Phys. Rev. Lett. **86**, 4843 (2001); J. Z. Liu, Q. Zheng, and Q. Jiang, Phys. Rev. B **67**, 075414 (2003).
[12] M. Arroyo and T. Belytschko, Phys. Rev. Lett. **91**, 215505 (2003).
[13] A. E. Cohen and L. Mahadevan, Proc. Natl. Acad. Sci. U.S.A. **100**, 12 141 (2003).
[14] M. Tuckerman, B. J. Berne, and G. J. Mantyna, J. Chem. Phys. **97**, 1990 (1992).
[15] D. W. Brenner, O. A. Shenderova, J. A. Harrison, S. J. Stuart, B. Ni, and S. B. Sinnott, J. Phys. Condens. Matter **14**, 783 (2002); D. W. Brenner, Phys. Rev. B **42**, 9458 (1990); J. Tersoff, Phys. Rev. B **38**, 9902 (1988).
[16] L. A. Girifalco, M. Hodak, and R. S. Lee, Phys. Rev. B **62**, 13 104 (2000).
[17] S. A. Nose, J. Chem. Phys. **81**, 511 (1984); W. G. Hoover, Phys. Rev. A **31**, 1695 (1985).
[18] A. Maiti, Chem. Phys. Lett. **331**, 21 (2000).
[19] M.-F. Yu, M. J. Dyer, J. Chen, D. Qian, W. K. Liu, and R. S. Ruoff, Phys. Rev. B **64**, 241403 (2001); B. Liu, M.-F. Yu, and Y. Huang, Phys. Rev. B **70**, 161402 (2004).
[20] B. I. Yakobson, M. P. Campbell, C. J. Brabec, and J. Bernholc, Comput. Mater. Sci. **8**, 341 (1997); M. A. L. Marques, H. E. Troiani, M. Miki-Yoshida, M. Jose-Yacaman, and A. Rubio, Nano Lett. **4**, 811 (2004); K. Asaka and T. Kizuka, Phys. Rev. B **72**, 115431 (2005).
[21] A. G. Rinzler, J. H. Hafner, P. Nikolaev, L. Lou, S. G. Kim, D. Tománek, P. Nordlander, D. T. Colbert, and R. E. Smalley, Science **269**, 1550 (1995).